

# Changes in extreme precipitation in the Huang-Huai-Hai River basin of China during 1960–2010

Dong-Dong Zhang · Deng-Hua Yan · Yi-Cheng Wang ·  
Fan Lu · Di Wu

Received: 30 May 2013 / Accepted: 15 April 2014 / Published online: 3 May 2014  
© Springer-Verlag Wien 2014

**Abstract** With the increasing exposure of populations and economy to the natural hazards, it is of vital importance to study the spatiotemporal characteristics of extreme precipitation. Based on daily precipitation at 154 meteorological stations in the Huang-Huai-Hai River basin of China during 1960–2010, the spatial and temporal changes in extreme precipitation were analyzed using twelve indices. The basin was divided into five climate areas using clustering analysis to detect the spatial changes of the extreme indices, and the temporal changes in the probability distributions of the extreme indices were also examined. The results showed that maximum 5-day precipitation, wet days and consecutive wet days decreased significantly while consecutive dry days showed a weak increasing trend. The other precipitation indices had insignificant decreasing trends. The probability distribution functions of simple daily intensity index and consecutive dry days were positively shifted while the rest of the indices were negatively shifted. The temporal changes of extreme indices implied that the frequency of extreme precipitation was decreasing, but the intensity of extreme precipitation was increasing in the Huang-Huai-Hai River basin. The spatial changes in the aspect of precipitation extreme events showed obvious spatial differences between different climate areas. In addition, the series including maximum 1-day precipitation and maximum 5-day precipitation were fitted by generalized extreme-value distribution for risk analysis and the results showed that the generalized extreme-value distribution could fit the series well. The amounts of extreme precipitation for different return periods were calculated and high risk areas for flooding disaster were presented.

## 1 Introduction

Recently, extreme weather and climate events have become more frequent than ever before due to climate warming, which has a significant impact on human society and even causes serious losses to people's lives and property (Fu et al. 2013; Goudie 2006; Groisman et al. 2013; Jhajharia et al. 2012; Kunkel et al. 1999; Martinez et al. 2012; Pittock et al. 2006; Suppiah and Hennessy 1998). The changes in the magnitude and frequency of extreme events are associated with the spatial and temporal characteristics in extreme precipitation as they may trigger floods and droughts (Shao et al. 2013). The fourth IPCC assessment report pointed out that the frequency and intensity of extreme precipitation in many areas showed an increasing trend, which drew concerns from meteorologists and hydrologists of the world (Dash et al. 2012; Gaffin et al. 2004; Stock et al. 2011).

Recently, precipitation extremes have been studied across different geographic regions and timescales (Bartholy and Pongrácz 2007, 2010; Cavalcanti 2012; Dodla and Ratna 2010; Hidalgo-Muñoz et al. 2011; Trambly et al. 2012; Zhang et al. 2012). Sheffield and Wood (2008) found that the precipitation extremes have already been amplified due to climate changes in some regions of Africa. Easterling et al. (2000) indicated that though the total precipitation may decrease or be unchanged, more extreme precipitation events had occurred over large areas of land especially in the midland high-latitude regions including Eastern Russia, Norway, and the north of Japan. Although the evidence for increasing trends appears in most regions, statistically decreasing trends in extreme rainfall events have been found in Western Australia (Haylock and Nicholls 2000), Southeast Asia and parts of the central Pacific (Griffiths et al. 2003; Manton et al. 2001), northern and eastern New Zealand (Salinger and Griffiths 2001), and in Poland (Bielec 2001). These studies have concluded that the changes in the aspect of precipitation extreme events showed obvious spatial differences.

D.-D. Zhang · D.-H. Yan (✉) · Y.-C. Wang · F. Lu · D. Wu  
State Key Laboratory of Simulation and Regulation of Water Cycle  
in River Basin, China Institute of Water Resources and Hydropower  
Research, 1-A Fuxing Road Haidian District Beijing 100038,  
People's Republic of China  
e-mail: denghuay@gmail.com

In China, Zhai et al (2005) have studied the trends in annual and seasonal total precipitation and in extreme daily precipitation (defined as those larger than its 95th percentile for the year) during 1951–2000 with 740 stations in China. The results indicated that there was little trend in total precipitation for China as a whole, but there were distinctive regional and seasonal patterns of trends. Several subsequent studies showed a rising trend in the occurrence of extreme precipitation events in the western part of Northwest China, the middle and lower reaches of the Yangtze River, South China and the Tibetan Plateau and a significant decrease trend in north China and the Sichuan Basin (Wang et al. 2008). Furthermore, based on the data of CDD (the maximum number of consecutive dry days) and CWD (the maximum number of consecutive wet days), Zhang et al (2011) have demonstrated that increasing fractional contribution of shorter consecutive wet days may imply intensifying precipitation in China. Many researchers analyzed the trend of extreme precipitation events with a threshold value in the past 50 years which showed a significant increasing trend in mean extreme precipitation days. Xia et al. (2011) examined changes in extreme precipitation events in the Huai River Basin and found insignificant increase in annual maximum rainfall and extreme precipitation events. In the case of Northeast China, Wang et al. (2013a, b, c) have demonstrated an overall decreasing trend in the frequency of extreme precipitation and the change patterns were not spatially clustered. However, few studies on changes in extreme precipitation conducted detailed analyses over the Huang-Huai-Hai River basin, even though it is a region that could be significantly impacted by possible future changes in climate. And there are limitations in using the comprehensive indices to analyze precipitation extreme events in the Huang-Huai-Hai River basin.

The objectives of this study are (1) to quantify spatial and temporal changes in extreme precipitation during 1960–2010 over the Huang-Huai-Hai River basin in China based on 12 indices; (2) to analyze the trends of the extreme precipitation in different climate areas and to identify if the considered area is getting more extreme in terms of precipitation; (3) to predict the extreme precipitation for different return periods by the generalized extreme value (GEV) distribution to provide basic data for the risk assessment of disasters in this area.

## 2 Materials and methods

### 2.1 Study area

Located in 30°–43° N, 100°–123° E as shown in Fig. 1, the Huang-Huai-Hai River basin usually refers to three sub-river basins, namely the Yellow River basin, Huai River basin, and Hai River basin including 13 provinces and two municipalities: Qinghai, Sichuan, Gansu, Ningxia, Inner Mongolia, Shaanxi, Shanxi, Henan, Hebei, Shandong, Anhui, Jiangsu,

Beijing, and Tianjin. The geography of the study area varies from west to east which consists of the Qinghai-Tibet Plateau, Inner Mongolia plateau, the Loess Plateau, and the Huang-Huai-Hai Plain with an area of  $1.445 \times 10^6 \text{ km}^2$  (Table 1). The plain area is  $5.24 \times 10^6 \text{ km}^2$  and the mountainous area covers  $0.921 \times 10^6 \text{ km}^2$ . Due to a vast territory, the climate in this area is influenced by many factors and can be classified as four types including temperate continental, temperate monsoon, subtropical monsoon, and highland climates. The precipitation, in general, decreases from south to north and from east to west and the average annual precipitation is 556.0 mm. As the main agricultural area and quick economic development area, the Huang-Huai-Hai watershed accounts for 25 % of the total GDP in China. However, frequent droughts and floods in this area had caused serious losses to the agriculture and industry recently (Du et al. 2014; Liu et al. 2008; Wang et al. 2011). Therefore, studies in assessing and predicting the influence of extreme precipitation are essential to offer theoretical and technical support for the water resource management and comprehensive response to extreme meteorological disasters.

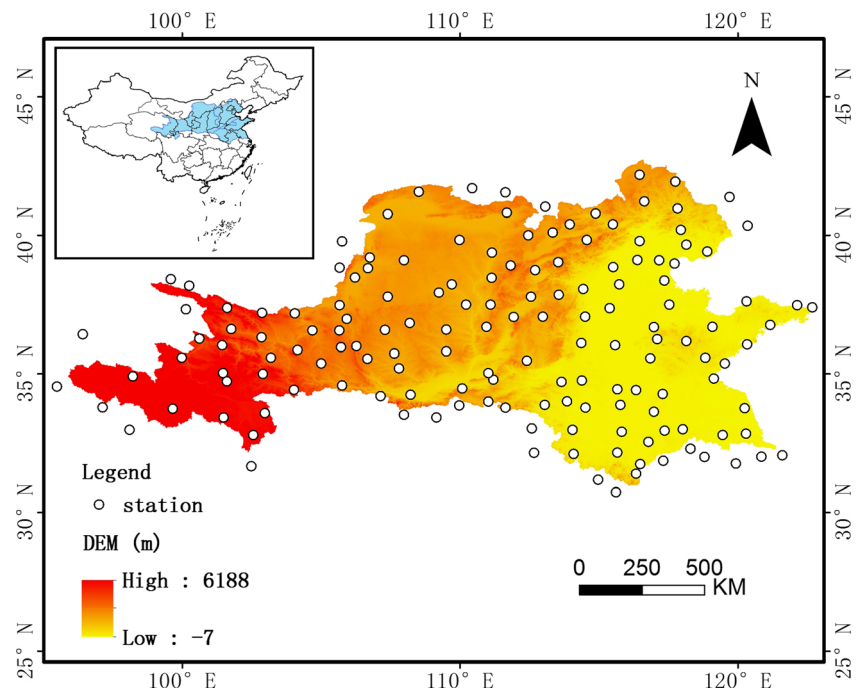
### 2.2 Data

There are 173 meteorological stations in Huang-Huai-Hai River basin. On the basis of the length of records, 159 meteorological stations are selected. Daily precipitation data of 159 stations in the Huang-Huai-Hai River basin is collected from the National Meteorological Information Center of China Meteorological Administration (CMA). The time series is from January 1960 to December 2010. Before constructing the precipitation indices series, data quality control and homogeneity assessment have to be performed on the initial data set of daily precipitation amounts from each station.

The RclimDex (<http://www.pcic.uvic.ca/tools-and-data/climdex>) which was developed by Xuebin Zhang at the Climate Research Branch of the Environment Canada was used for data quality control. The precipitation values which were below 0 mm would be taken as missing values. The outliers were defined as the mean value of the year plus or minus four times the standard deviation of the value for that calendar day in this study (Tian et al. 2012). If the values were outside the thresholds, they were marked as potentially erroneous. The potentially erroneous values were checked and set to missing values. We completed the missing data through the average precipitation values of the neighboring stations, which had been used to reconstruct the missing precipitation data in the Hai River Basin and proved to be effective (Wang et al. 2011).

Climate data series usually contain artificial shifts due to inevitable changes in observing instrument (or observer), location, environment, and observing practices/procedures taking place in the period of data collection (Cao and Yan 2012). It is important to detect artificial shifts in climate data series, because these artificial changes could considerably bias

**Fig. 1** Study area and location of the meteorological stations



the results of climate trends, variability, and extremes analysis. To eliminate the possible effect of artificial shifts caused by relocations of measurement sites or other unknown reasons, the time series of daily precipitation in Huang-Huai-Hai River basin from each station was checked for temporal homogeneity using the software package RHtestsV3. The results revealed that no shifts had been detected in the data sets for all the stations except five stations. After rejecting five stations with inhomogeneous series, 154 stations were finally selected in this study (Fig. 1). There are 78 stations located in the Yellow River basin, 44 stations in the Huai River basin, and 32 stations in the Hai River basin.

2.3 Climate areas

The basin is divided into five climate areas (Fig. 2, Table 2) using clustering analysis via the self-organizing map (SOM) neural network algorithm based on the data of the latitude and longitude (i.e., *X* and *Y* geodetic coordinate values), elevation, and annual average precipitation of the 154 meteorological stations. Compared with other classification methods, SOM is

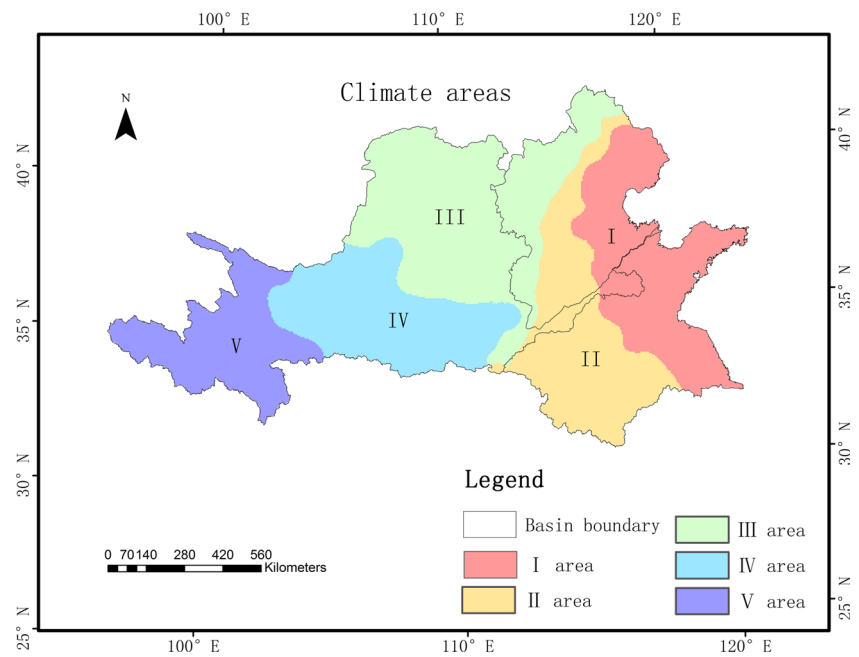
a network capable of self-organization and self-learning; and its other advantages include that it realizes real-time learning, possesses network stability, does not require external evaluation functions, recognizes the most significant characteristics of the vector space, has good anti-noise ability, and etc. (Yan et al. 2013; Yang and Yan 2006).

In area I, there are 32 representative meteorological stations, accounting for 21 % of the total number of stations, which are mainly distributed in the area surrounding Bo Sea and the Shandong Peninsula as well as the downstream of Huai River. Area II has 33 stations, accounting for 21 %, which are mainly distributed in the upper and middle reaches of the Huai River as well as the Daqing River, Ziya River, and Zhangwei River plains in the Hai River basin. Area III has 38 stations, accounting for 25 %, which are mainly distributed on the Hetao Plain in Ningxia-Inner Mongolia and Inner Mongolia Plateau, the Fen-Wei Valley basin in Shanxi and Shaanxi Provinces as well as on the Loess Plateau. Area IV has 28 representative meteorological stations, accounting for 18 %, which are mainly located in the high mountains and hilly regions at altitudes of 1,500–3,000 m. And in area V, there are 23 stations, accounting for 15 %, which

**Table 1** Area of sub-River basin and the characteristic of precipitation (1961–2010)

River basin	Total area ( $1 \times 10^6$ km <sup>2</sup> )	Annual precipitation		
		Mean value/mm	Range/mm	Coefficient of variation
Hai	0.320	538.1	481.3	0.18
Yellow	0.795	439.9	325.9	0.14
Huai	0.330	854.2	631.8	0.16
Huang-Huai-Hai	1.445	556.0	389.3	0.12

**Fig. 2** Climate areas in Huang-Huai-Hai River basin



are mainly located on the Tibetan Plateau in the Yellow River basin at altitudes above 3,000 m.

## 2.4 Methodology

In this paper, the Mann–Kendall test method was employed to test the significance of trends (at the 95 % level of confidence in the study), and the annual trend rates were calculated using Kendall slope estimator (Akritas et al. 1995). Regional averages were calculated as an arithmetic mean of values at all stations in the study and the correlations among these indices were also analyzed. The number of stations with the same trend as that for the whole region had been counted for each index, and stations with significant trends had also been identified. In addition, the weighted 11-year binomial moving average was used to show the interannual variation of climatic extremes (Böhm et al. 2001). Factor analysis was used to partition the data set into clusters with in-cluster similarities and between-cluster dissimilarities (Li et al. 2011). The generalized extreme value distribution (GEV) was used to model

the extreme precipitation distributions and predict the extreme precipitation for different return periods.

### 2.4.1 Extreme precipitation indices

The Expert Team on Climate Change Detection and Indices (ETCCDI) defined 27 core extreme indices based on daily temperature and precipitation. Exact definitions of all the indices are available from the ETCCDI website ([www.clivar.org/organization/etccdi/etccdi.php](http://www.clivar.org/organization/etccdi/etccdi.php)). In this study, twelve indices (Table 3) which can reflect the changes of extreme precipitation in different aspects are chosen. An R-based program, RCLimDexV3 developed at the Climate Research Branch of the Meteorological Service of Canada, is applied to calculate these extreme indices. The precipitation indices are divided into two types. One is precipitation indices including maximum 1-day precipitation, maximum 5-day precipitation, very wet day precipitation, extremely wet day precipitation, and simple daily intensity. The other is the number of days with precipitation including wet days, consecutive wet days, consecutive dry days,

**Table 2** Basic information of climate areas in the study area

Climate areas	Climate types	Number of meteorological stations	Ratio (%)
I	Subtropical monsoon climate	32	21
II	Temperate monsoon climate	33	21
III	Temperate continental climate	38	25
IV	Temperate continental climate	28	18
V	Plateau mountain climate	23	15

**Table 3** Definition of extreme climate indices

Acronym	Name of the index	Definition	Units
RX1DAY	Maximum 1-day precipitation	Annual maximum 1-day precipitation	mm
RX5DAY	Maximum 5-day precipitation	Annual maximum consecutive 5-day precipitation	mm
R95T	Very wet day precipitation	Annual total precipitation when RR >95th percentile of 1960–2010 daily rainfall	mm
R99T	Extremely wet day precipitation	Annual total precipitation when RR >99th percentile of 1960–2010 daily rainfall	mm
PRCPTOT	Wet day precipitation	Annual total PRCP in wet days (RR ≥ 1 mm)	mm
SDII	Simple daily intensity index	Average precipitation on wet days	mm/day
R10mm	Number of heavy precipitation days	Annual count of days when RR ≥ 10 mm	days
R20mm	Number of very heavy precipitation days	Annual count of days when RR ≥ 20 mm	days
R30mm	Number of extremely heavy precipitation days	Annual count of days when RR ≥ 30 mm <sup>a</sup>	days
NW	Wet days	Annual count of days when RR ≥ 1 mm	days
CDD	Consecutive dry <sup>b</sup> days	Maximum number of consecutive dry days	days
CWD	Consecutive wet <sup>c</sup> days	Maximum number of consecutive wet days	days

<sup>a</sup> 30 mm was the threshold defined by the authors  
<sup>b</sup> Dry days are those days when the amount recorded was < 1 mm  
<sup>c</sup> Wet days are those days when the amount recorded was ≥ 1 mm

heavy precipitation days, very heavy precipitation days, and extremely heavy precipitation days.

2.4.2 Mann–Kendall trend test

In this study, the Mann–Kendall (MK) statistical test (Mann 1945), a nonparametric approach, is applied to characterize the trends for the twelve indices and to test their significance. The Mann–Kendall test is a rank-based procedure, which is less sensitive to outliers than parametric approaches and it is widely used in hydrology and climatology (Hamed 2009; Tian et al. 2012; Wang et al. 2008).

In the MK test, the test statistic is calculated as follows:

$$S = \sum_{k=1}^{n-1} \sum_{j=k+1}^n \text{sgn}(x_j - x_k) \tag{1}$$

where

$$\text{sgn}(x_j - x_k) = \begin{cases} 1 & \text{if } x_j - x_k > 0 \\ 0 & \text{if } x_j - x_k = 0 \\ -1 & \text{if } x_j - x_k < 0 \end{cases} \tag{2}$$

$x_j$  and  $x_k$  are the sequential data values,  $n$  is the length of the data series, and the normally distributed variate  $z$  is computed as follows:

$$z = \begin{cases} \frac{S-1}{\text{Var}(S)} & \text{if } S > 0 \\ 0 & \text{if } S = 0 \\ \frac{S+1}{\text{Var}(S)} & \text{if } S < 0 \end{cases} \tag{3}$$

$$\text{Var}(S) = \frac{n(n-1)(2n+5) - \sum t(t-1)(2t+5)}{18} \tag{4}$$

$\text{Var}(S)$  is the variance of the test statistic  $S$  (Hamed 2009) and  $t$  is the extent of any given tie. A tie is the sample data having the same value and the summation is over all ties (Hirsch et al. 1982). The null hypothesis is that a series  $x_1, \dots, x_n$  is independent and identically distributed. At the 95 % confidence level, if  $|z| > 1.96$ , the null hypothesis of no trend is rejected.

In Mann–Kendall test, another very useful index is the Kendall slope, which is the magnitude of the monotonic change and is given as follows:

$$\beta = \text{Median} \left( \frac{x_j - x_i}{j - i} \right) \quad \forall j < i \tag{5}$$

In which  $1 < i < j < n$ : The estimator  $\beta$  is the median over all combination of record pairs for the whole data set.

2.4.3 The generalized extreme value distribution

The generalized extreme value (GEV) distribution is widely employed for modeling extremes in the meteorology and many other fields (Coles et al. 2003; Khaliq et al. 2006; Lu et al. 2013). It was introduced into meteorology by Jenkinson (1955) and is used extensively to model extremes of natural phenomena such as precipitation (Gellens 2002), temperature (Nogaj et al. 2007), and wind speed (Coles and Casson 1998). The GEV distribution is a family of continuous probability distributions developed to combine the Gumbel, Fréchet, and

Weibull families. The distribution function of the GEV distribution is as follows:

$$F(x) = \begin{cases} \exp\left\{-\left[1 + \theta_3 \frac{(x-\theta_1)}{\theta_2}\right]^{-1/\theta_3}\right\}, & \theta_3 \neq 0, \\ \exp\left\{-\exp\left[-\frac{(x-\theta_1)}{\theta_2}\right]\right\}, & \theta_3 = 0, \end{cases} \quad (6)$$

where  $\theta_1$ ,  $\theta_2$  and  $\theta_3$  are the location parameter, the scale parameter, and the shape parameter, respectively,  $\theta_1 \in R, \theta_2 > 0, \theta_3 \in R$  and  $1 + \theta_3(x - \theta_1)/\theta_2 > 0$ .

### 3 Results

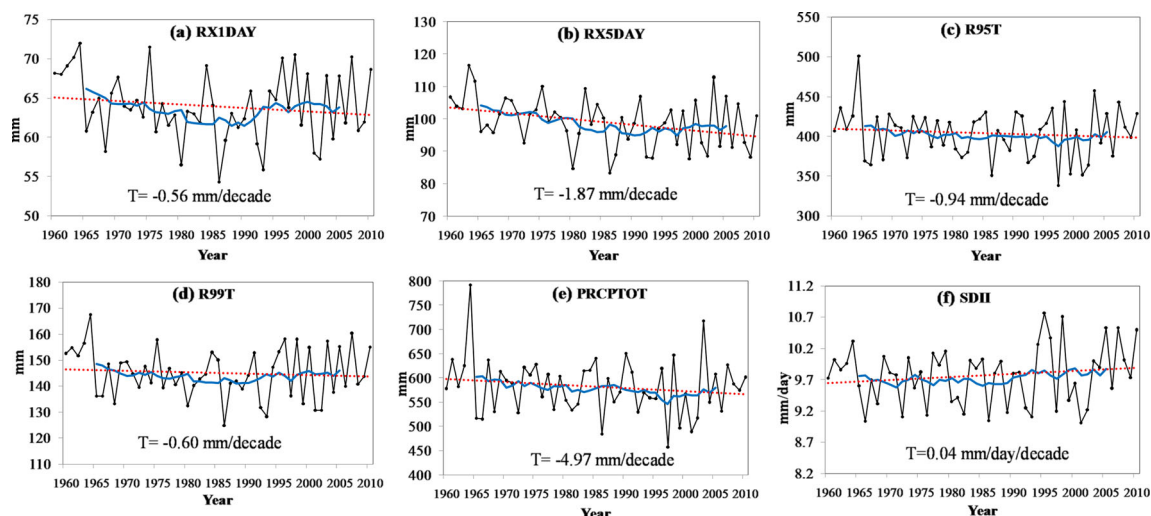
#### 3.1 Precipitation indices

Figure 3 shows the regional annual series for precipitation indices in the Huang-Huai-Hai River basin during 1960–2010, and Fig. 4 demonstrates the spatial distribution pattern of temporal trends in precipitation extremes for the 154 meteorological stations. Table 4 shows the results of Mann–Kendall test. Percentages of stations which show positive (negative) trend and significant positive (negative) trend are also present in Table 4. Table 5 gives an overview of percentages of stations with the same trend as the study area for precipitation indices in different climate areas. Regional averages of maximum 1-day precipitation (RX1DAY) had no significant decreasing trends with fluctuations during 1960–2010 over the study region (Fig. 3a). About 51.6 % of the stations, most of which were located in the areas I, III, and IV, showed decreasing trends, but some stations in the Huai River

basin and upper Yellow River basin (mainly in areas II and V) displayed increasing trends (Fig. 4a). The trend pattern of maximum 5-day precipitation (RX5DAY) resembles closely that of maximum 1-day precipitation (RX1DAY) in Figs. 3b and 4b. Regional averages of RX5DAY had significant decreasing trends with 57.8 % of the stations showing negative trend (Table 4), most of which were in the areas I, III, and IV.

The regional average trends of very wet day precipitation (R95T) and extremely wet day precipitation (R99T) had weak decreasing trends from 1960 to 2010 (Fig. 3c, d). The proportion of stations with negative trend was 52.6 and 47.4 %, respectively. The proportion of stations showing significant negative trends was 3.2 % for both of the indices (Table 4). For the R95T index, the largest decreasing trends were observed in the Hai River basin, Yellow River basin, and the eastern part of Huai River basin (Fig. 4c), and the increasing trends were detected in the west of Huai River basin and the northwest of area V (Fig. 4d). Decreasing and increasing regions for R99T were almost the same as the regions for R95T.

The wet day precipitation (PRCPTOT) had no significant decreasing trends and mean precipitation amount on a wet day (SDII) had increased slightly during 1960–2010 (Fig. 3e, f). The trend rate of PRCPTOT varied from  $-64.21$  to  $37.63$  mm/decade, and 64.3 % of stations had decreasing trends, particularly in the areas I, III and IV (Fig. 4e). As to SDII, most of the study areas increased except the northern part of the Hai River basin and the central region of the Yellow River basin (Fig. 4f). The index of SDII is dependent on two variables, namely total annual precipitation and number of wet days. As is shown in Fig. 7d, almost the whole region is dominated by negative trend of NW, and the areas with decreasing SDII should be characterized by a stronger negative trend rate of total annual precipitation than that of NW.



**Fig. 3** Interannual variation of precipitation extremes in Huang-Huai-Hai River basin during 1960–2010 (The dotted red line is the linear trend, the blue line is the 11-year smoothing average, and  $T$  is the decadal trend rate)

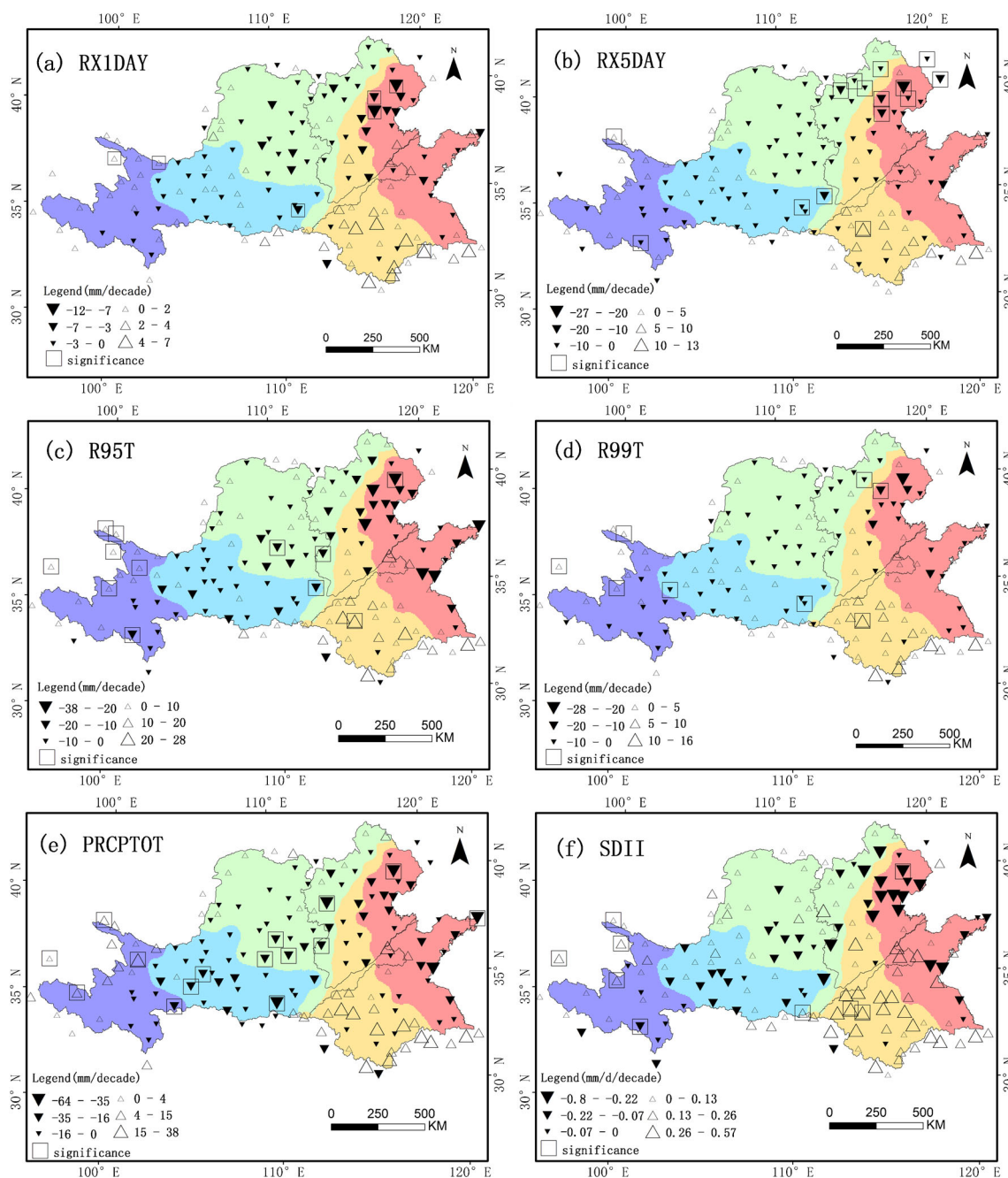


**Fig. 4** Spatial distribution of decadal trends in precipitation extremes in Huang-Huai-Hai River basin during 1960–2010

The contribution of extreme precipitation to total precipitation decreased for extremely wet day precipitation (R99T) while it increased for very wet day precipitation (R95T) between 1960 and 2010, indicating that very wet day precipitation (R95T) may reflect the variation in total wet day precipitation in the Huang-Huai-Hai River basin. This result is similar to that of the IPCC Fourth Assessment Report which indicates the increase in the proportion of total precipitation from heavy rainfall over most area (Climate Change 2007). Very wet days accounted for an average of 70.3 % of the total precipitation amount (range 43.4 to 87.7 %) (Fig. 5a). The

average contribution of extremely wet days was 25.2 % (range 17.6 to 32.3 %) (Fig. 5b).

### 3.2 Indices of days with precipitation

Over the period of 1960–2010, the regional average occurrence of heavy precipitation days (R10mm), very heavy precipitation days (R20mm), and extremely heavy precipitation days (R30mm), all had insignificant decreasing trends (Fig. 6 and Table 4). Wet days (NW) and consecutive wet days (CWD) had a significant decreasing trend while the

**Table 4** Results of the Mann–Kendall test and percentages of stations with positive or negative trends for regional indices of precipitation extremes in Huang-Huai-Hai River basin during 1960–2010

Index	Kendall slope	Range	Positive trend			Negative trend		
			Total	SS	Non-SS	Total	SS	Non-SS
Precipitation indices	(mm/decade)	(mm/decade)	%	%	%	%	%	%
RX1DAY	−0.56	−11.46 to 6.92	49.4	2.6	46.8	51.6	1.9	48.7
RX5DAY	−1.87*	−26.94 to 12.59	42.2	1.3	40.9	57.8	8.4	49.4
R95T	−0.94	−35.56 to 25.18	47.4	4.5	42.9	52.6	3.2	49.4
R99T	−0.60	−25.00 to 14.42	52.6	3.2	49.4	47.4	3.2	44.2
PRCPTOT	−4.97	−64.21 to 37.63	35.7	2.6	33.1	64.3	7.1	57.2
Precipitation indices	(mm/day/decade)	(mm/day/decade)	%	%	%	%	%	%
SDII	0.04	−0.80 to 0.57	62.9	4.5	58.4	37.0	1.3	35.7
Day indices	(day/decade)	(day/decade)	%	%	%	%	%	%
R10mm	−0.15	−2.42 to 0.95	43.5	1.3	42.2	56.5	3.9	52.6
R20mm	−0.04	−0.70 to 0.67	43.5	0.6	42.9	56.5	0.0	56.5
R30mm	−0.02	−0.59 to 0.44	40.9	0.6	40.3	59.1	5.2	53.9
NW	−0.81*	−7.83 to 2.00	15.6	1.3	14.3	84.4	18.8	65.6
CDD	0.05	−1.43 to 3.33	53.9	2.6	51.3	46.1	3.2	42.9
CWD	−0.11*	−0.49 to 0.25	21.4	0.0	21.4	78.6	8.4	70.2

SS statistical significance,  $\alpha=0.05$

\*Significant

consecutive dry days (CDD) showed an insignificant increasing trend. The spatial distributions of the changes in trends of the number days with precipitation were very different. For the index of R10mm, 56.5 % of stations showed decreasing trend, and only six stations were significant. The regions with decreasing trend were found in the Yellow River basin and the eastern coastal areas in the Hai River basin and Huai River basin (Fig. 7a). Similarly, for the indices of R20mm and

R30mm, more than half of the stations experienced a decrease (Table 4). Stations in areas I, III, and IV displayed decreasing trends (Fig. 7b, c). In case of the NW index, the negative trend was found in most part (84.4 % of the stations) of the Huang-Huai-Hai River basin (Fig. 7d, Table 5). Similar result was found while analyzing the CWD index. Up to 78.6 % of stations in the Huang-Huai-Hai River basin experienced a decrease especially in areas II, III, IV, and V (Fig. 7f). Changes in the consecutive dry days (CDD) further reinforce this pattern, with 53.9 % of stations having an increasing trend (mostly in areas I and II and the middle of Yellow River basin) with four stations significant at the 0.05 level (Fig. 7e).

In addition, the changes in trends of precipitation indices in different climate areas during 1960–2010 are further analyzed (Table 5). For most of the indices, more than 50 % of stations in areas I, III, and IV show the same sign of the trend as the study area. For the indices of SDII, NW, and CWD, more than 50 % of stations in areas II and V show the same sign of trend as the study area while for the other indices, the trend in areas II and V is opposite to that of the study area. For the indices of NW and CWD, more than 55 % stations in all the five climate areas show the same sign of trend as the study area, indicating that the influence of climate on the two indices was not obvious.

### 3.3 Patterns of distribution changes between 1960 and 2010

To further research the temporal changes in precipitation extremes, the probability distribution functions (PDFs) of

**Table 5** Percentages of stations with the same trend as the study area for precipitation indices in different climate areas during 1960–2010 (%)

	Regional trend	I (%)	II (%)	III (%)	IV (%)	V (%)
RX1DAY	D	62.5	24.2	73.7	57.1	21.7
RX5DAY	D	62.5	33.3	73.7	67.9	47.8
R95T	D	68.8	21.2	55.2	71.4	39.1
R99T	D	56.2	21.2	60.5	50.0	39.1
PRCPTOT	D	81.3	42.4	63.1	96.4	30.4
SDII	I	46.8	87.9	63.1	50.0	65.2
R10mm	D	75.0	30.3	55.2	85.7	34.8
R20mm	D	81.3	39.4	55.3	60.7	43.4
R30mm	D	71.9	42.4	71.0	75.0	26.1
NW	D	93.8	84.8	81.5	100	56.5
CDD	I	71.9	66.7	39.4	57.1	34.8
CWD	D	65.6	72.7	78.9	96.4	73.9

D indicates that the regional trend in Huang-Huai-Hai River basin has decreased, I indicates that the regional trend in Huang-Huai-Hai River basin has increased



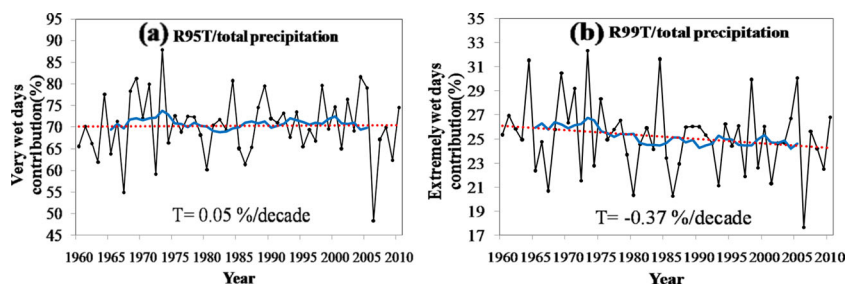


**Fig. 5** Regional series for **a** the ratio of the index of precipitation on very wet days (R95T) to total precipitation and **b** the ratio of the index of precipitation on extremely wet days (R99T) to total precipitation in the

Huang-Huai-Hai River basin during 1960–2010 (The dotted red line is the linear trend, the blue line is the 11-year smoothing average, and *T* is the decadal trend rate)

each index for two different time periods were calculated. The data have been split into two periods, i.e., 1960–1984 and 1985–2010. The probability density function plots are closely examined to determine if the distributions of two time periods are the same.

Figure 8 shows the PDFs for twelve indices for 1960–1984 and 1985–2010, respectively. The PDFs of two different time periods followed the same distributions for all the indices except RX5DAY and CWD. The shapes of the distributions for all the indices except CWD for 1985–2010 were smoother than those for 1960–1984. For RX5DAY and CWD, the distributions are significantly different between two periods with remarkable negative shifts. The PDFs of SDII and CDD were positively shifted, and the rest of the indices were negatively shifted. Generally, the distribution changes in precipitation indices showed a tendency toward drier conditions, which was in accord with the result of trends analysis above.

### 3.4 Analysis of correlations of precipitation indices

Factor analysis of the precipitation data revealed that F1, which included all precipitation indices accounted for

69.1 % of the overall variance (Table 6). This reflected the similarity of variations in annual precipitation and extreme precipitation events, and the increasing contribution made by very wet day precipitation to annual total precipitation. RX1DAY and CDD dominated F2, which accounted for 10.7 % of the total variance, confirming the decrease of RX1DAY and the increase of CDD were the main factors which influenced changes in annual precipitation.

Table 7 also showed that the correlations between extreme precipitation indices and total precipitation were significant at the 0.01 level except CDD. The correlation coefficients between the total precipitation and precipitation indices, including very wet day precipitation (R95T), heavy precipitation days (R10mm), very heavy precipitation days (R20mm), extremely heavy precipitation days (R30mm) exceeded 0.9, and the others exceeded 0.5, indicating that annual total precipitation was well correlated with extreme precipitation. Therefore, the indices selected in this study could reflect the changes in annual total precipitation. In addition, Table 7 also showed that there were statistically significant correlations among the precipitation indices. The result was in agreement with the findings of previous work (Wang et al. 2011; You et al. 2011).

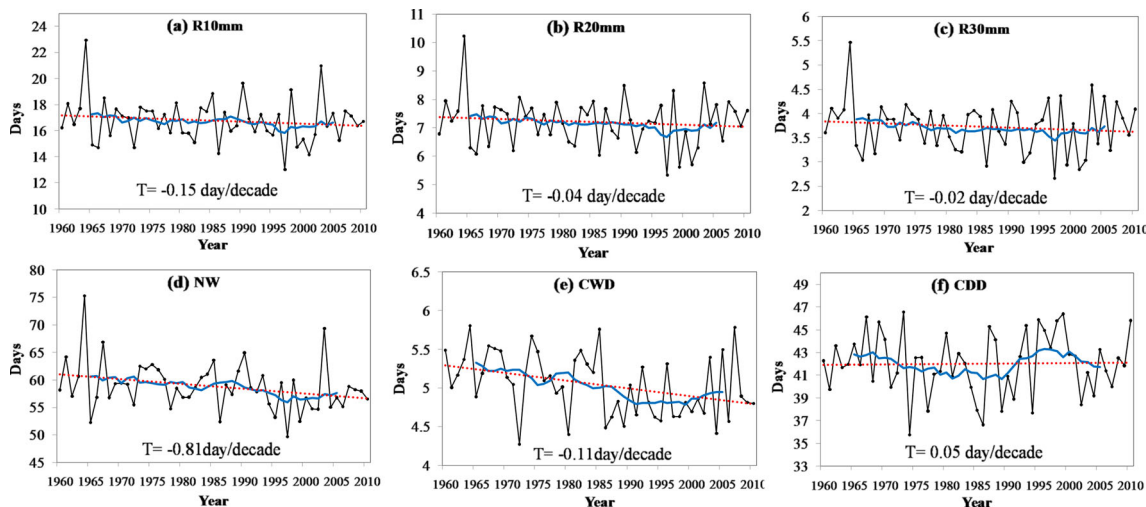


**Fig. 6** Interannual variation of precipitation extremes in Huang-Huai-Hai River basin during 1960–2010 (The dotted red line is the linear trend, the blue line is the 11-year smoothing average, and *T* is the decadal trend rate)

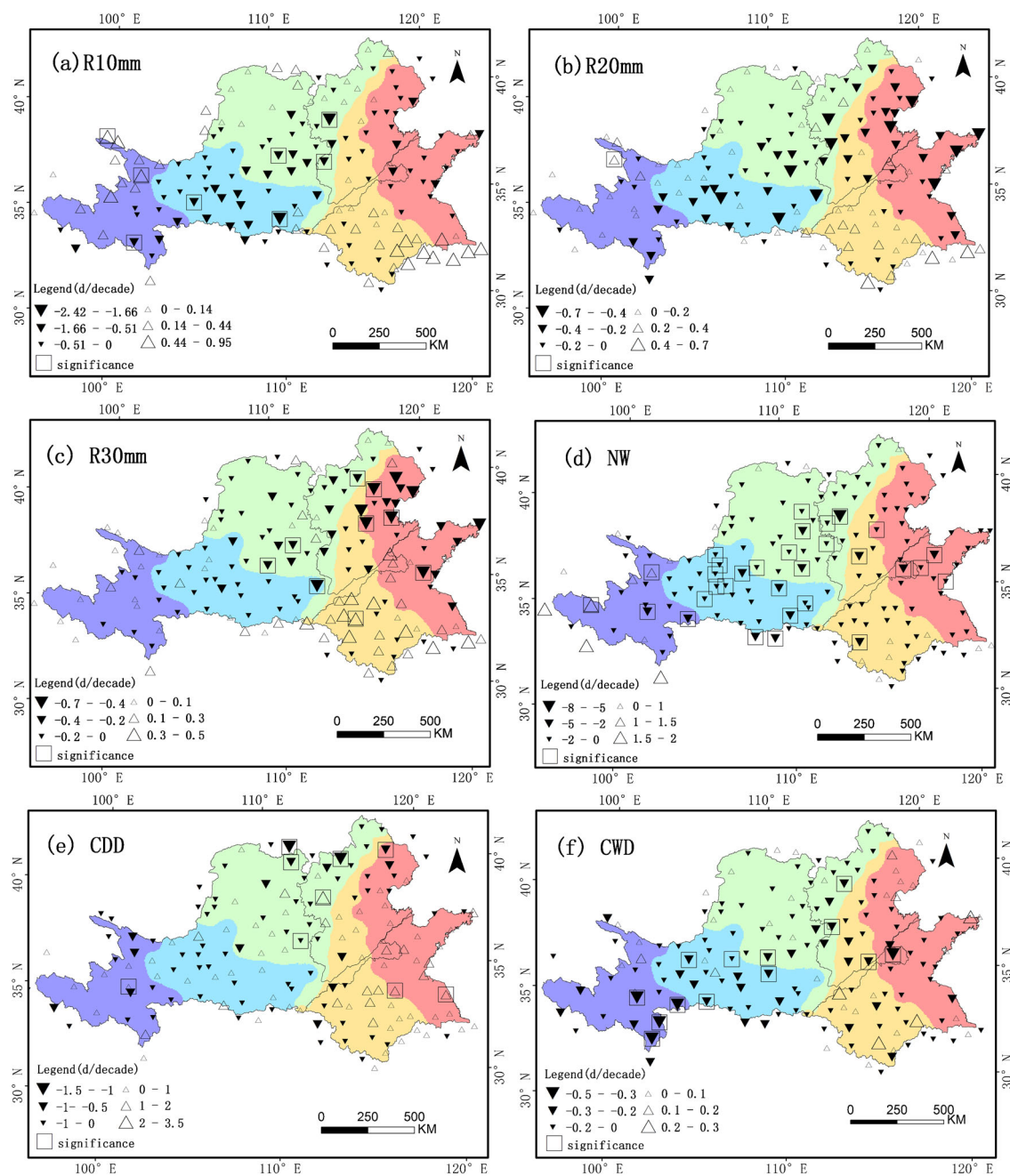


**Fig. 7** Spatial distribution of decadal trends in precipitation extremes in Huang-Huai-Hai River basin during 1960–2010

### 3.5 Estimation of extreme precipitation for different return periods

The series of maximum 1-day precipitation (RX1DAY) and maximum 5-day precipitation (RX5DAY) for each station were fitted by generalized extreme-value distribution (GEV), which was widely employed for modeling extremes in the meteorology (Lu et al. 2013). The parameters of the distributions were estimated using maximum likelihood method. The goodness of fit of the probability

function was evaluated by Kolmogorov–Smirnov’s statistic  $D$  (K–S  $D$ ) at 95 % confidence level (Frank and Masse 1951). Results showed that all the series passed the K–S test and GEV can be used to describe the distributions of the series of RX1DAY and RX5DAY. According to the amount of precipitation, estimates of extreme precipitation indices for different return periods were clarified into six classes using natural break method and indicated by different colors in the map (Fig. 9). It showed that the amount of extreme precipitation reduces gradually from

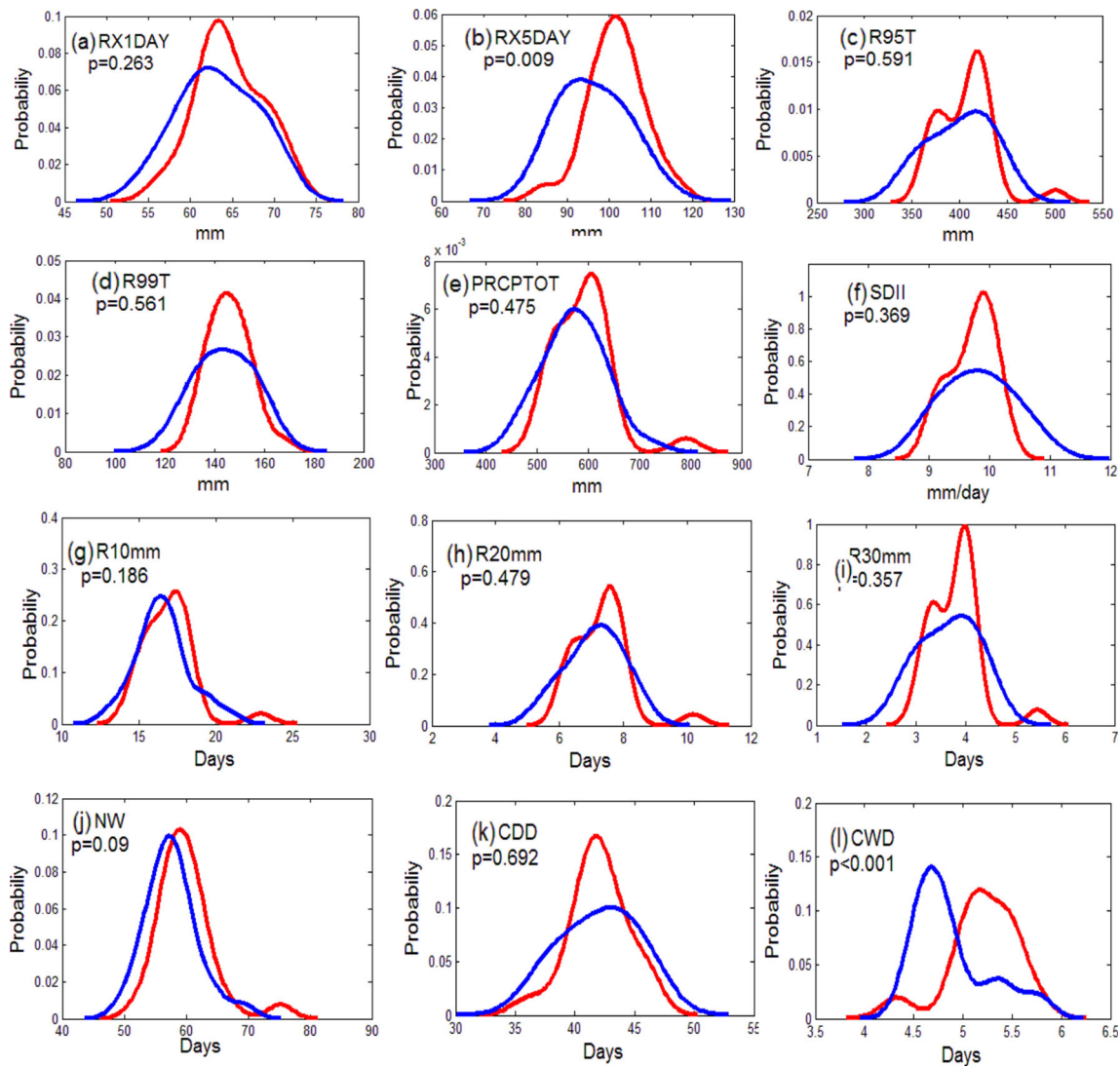


**Fig. 8** Annual PDFs of the extreme precipitation indices for the two sub-periods, 1960–1984 (red line) and 1985–2010 (blue line), and  $P$  value  $<0.05$  means that the hypothesis of Kolmogorov–Smirnov and the two distributions are the same and can be rejected

the east to the west. For the RX1DAY for different return periods, large amount of precipitation was detected in the upper reaches and the eastern part of Huai River basin. For the RX5DAY for return periods of 50 years, the precipitation in many areas including the upper reaches and the eastern part of the Huai River, parts of Hebei province, and the city of Zhengzhou would exceed 250 mm/day which may lead to flash flood and urban pluvial flood.

#### 4 Discussion and conclusion

Based on observed data from 154 meteorological stations in the Huang-Huai-Hai River basin of China during 1960–2010, 12 indices of extreme precipitation were employed to analyze the spatial and temporal distributions of precipitation extremes. And the main findings are summarized as follows:

Most part of the Huang-Huai-Hai River Basin showed mixed positive and negative trends in the precipitation

**Table 6** Factor loadings of the variance of precipitation indices

Factors	Total P	RX1DAY	RX5DAY	R95T	R99T	PRCPTOT	SDII	R10mm	R20mm	R30mm	NW	CDD	CWD	%Variance
F1	0.97	0.77	0.75	0.98	0.89	0.97	0.73	0.91	0.95	0.96	0.81	0.06	0.57	69.1
F2	-0.20	0.49	0.25	0.04	0.37	-0.19	0.44	-0.33	-0.14	0.02	-0.49	0.54	-0.17	10.7

**Table 7** Correlation coefficients of precipitation extremes

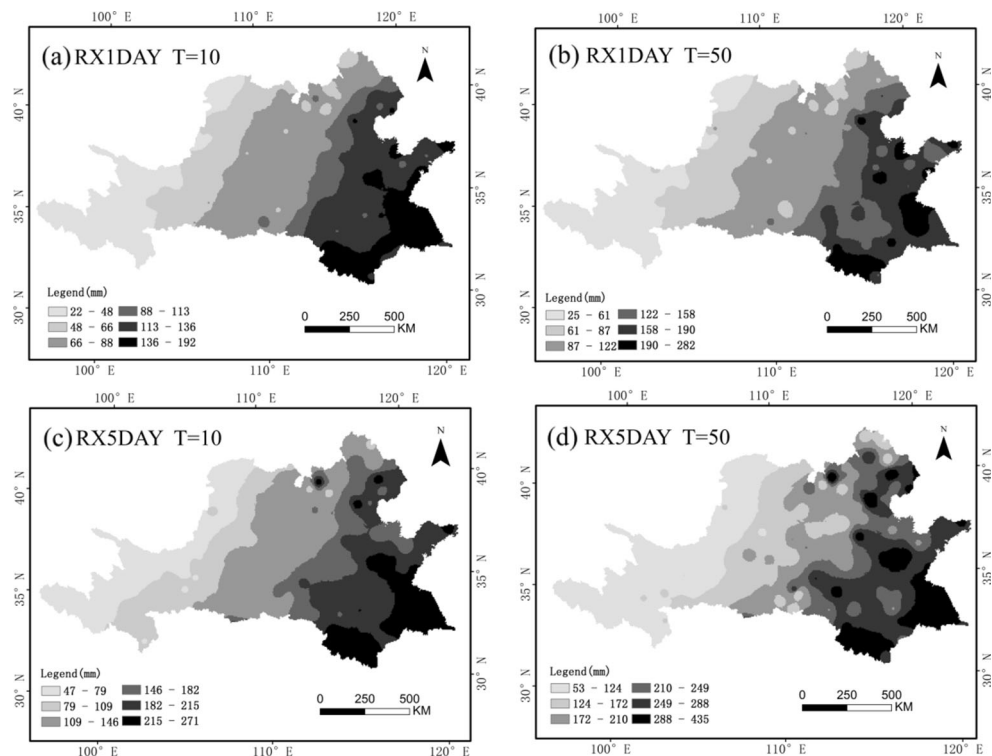
	Total <i>P</i>	RX1DAY	RX5DAY	R95T	R99T	PRCPTOT	SDII	R10mm	R20mm	R30mm	NW	CDD	CWD
Total <i>P</i>	1												
RX1DAY	0.65*	1											
RX5DAY	0.63*	0.80*	1										
R95T	0.94*	0.74*	0.68*	1									
R99T	0.80*	0.94*	0.81*	0.90*	1								
PRCPTOT	1*	0.64*	0.63*	0.96*	0.79*	1							
SDII	0.67*	0.66*	0.49*	0.80*	0.78*	0.63*	1						
R10mm	0.95*	0.49*	0.51*	0.89*	0.65*	0.97*	0.57*	1					
R20mm	0.95*	0.58*	0.54*	0.96*	0.75*	0.96*	0.72*	0.95*	1				
R30mm	0.92*	0.70*	0.64*	0.98*	0.85*	0.94*	0.78*	0.88*	0.96*	1			
NW	0.85*	0.42*	0.51*	0.73*	0.54*	0.89*	0.26	0.90*	0.80*	0.73*	1		
CDD	-0.03	0.14	-0.01	0.06	0.12	0.02	0.17	0.00	0.06	0.08	-0.05	1	
CWD	0.50*	0.44*	0.62*	0.47*	0.45*	0.52*	0.23	0.50*	0.43*	0.43*	0.56*	-0.04	1

\*Significant at the 0.01 level

extreme indices, but most of these trends were not significant. For the regional average trends of precipitation extremes, SDII and CDD had insignificant increasing trends while the other indices, including RX1DAY, RX5DAY, R95T, R99T, PRCPTOT, R10mm, R20mm, R30mm, NW, and CWD had decreasing trends, and RX5DAY, NW, and CWD were statistically significant. The regional average annual total precipitation (PRCPTOT) trend for the whole region was negative

but statistically insignificant at the 95 % confidence level, which had been revealed in the regional studies (Wang et al. 2013a, b, c; Zhai et al. 2005). The decreasing trends in indices of NW, R10, R20, R30, and CWD dominated for a majority of the study area which indicated that the frequency and duration of extreme precipitation in the study area were decreasing. This climatic evolution is consistent with the results of the trend analyses in precipitation performed in the study area

**Fig. 9** Amounts of RX1DAY and RX5DAY for return periods of 10 and 50 years in Huang-Huai-Hai River basin



(Du et al. 2014; Liu et al. 2008; Wang et al. 2011). Further study on the changes of distribution for all the indices between 1960 and 2010 confirmed the conclusion above. In addition, the contribution of extremely wet precipitation (R99T) to total precipitation decreased and while it increased for very wet day precipitation (R95T) between 1960 and 2010, indicating that R95T may reflect the variation in total wet day precipitation in the Huang-Huai-Hai River basin.

The study areas were divided into five different climate areas using SOM. The change patterns for different climate areas were different. For the area I, all the indices had decreasing trends except CDD, indicating a decrease in both intensity and frequency of extreme precipitation in this area. For the area III, all the indices had decreasing trends except SDII, indicating a decrease in frequency but an increase in intensity of extreme precipitation in this area. Similar results were found in area IV, the indices of CDD and SDII in area IV had increased while the other indices had decreased. For the area II, all the indices had increased except CWD and NW. Similar results were found in area V with the increased indices of CWD, NW, and CDD. The results might indicate that more total extreme precipitation was accompanied by more extremes precipitation amount and less days of extremes precipitation in areas II and V. For the indices of NW and CWD, more than 55 % stations in all the five climate areas showed the same sign of trend as the study area which indicated that the influence of climate on the two indices was not obvious. Overall, the changes in trends of indices implied that the frequency of extreme precipitation was decreasing but the intensity of extreme precipitation was increasing in the Huang-Huai-Hai River basin.

In the time series of these extreme precipitation indices, most of precipitation indices were strongly correlated with annual total precipitation in the Huang-Huai-Hai River basin. Factor analysis of the precipitation data revealed that the decrease of RX1DAY and the increase of CDD were the main factors which influenced changes in annual precipitation. Extreme precipitation indices including RX1DAY and RX5DAY for different return periods were calculated by GEV and high risk is detected in the upper reaches and the eastern part of the Huai River, parts of Hebei province, and the city of Zhengzhou which would exceed 250 mm/day for annual maximum consecutive 5-day precipitation.

Some characteristics of precipitation extremes are obtained based on statistical analysis. The results of this study may provide some valuable information of regional precipitation change in the study area. However, the uncertainty of spatial distribution may be induced by many factors including systematic errors in the interpolation and areal average method, stochastic error due to the random nature of precipitation and the density of the meteorological stations. The uncertainty of temporal distribution may be induced by climate changes and human activities. There is indeed mounting evidence that

hydroclimatic extreme series are not stationary, owing to natural climate variability or anthropogenic climate change (Coles et al. 2003). The series of RX5DAY, which were fitted by generalized extreme-value distribution, could be nonstationary as shown in Fig. 8. Therefore, there will be uncertainty in the estimation of extreme precipitation for different return periods as we use stationary GEV model. Further work should be done to build a nonstationary GEV model for better understanding the distributions of the extreme precipitation. For the above-discussed reasons, this study confirmed the complexity and uncertainty of the spatial and temporal variability of extreme precipitation and the importance of gathering local information to obtain a reliable and detailed description of characteristics and dynamics of extreme precipitation at the regional level. Furthermore, in the context of accelerating warming and water circulation, relationships between changes in temperature extremes and attendant changes in precipitation extremes should be considered, since the two types of extremes are not necessarily independent.

**Acknowledgments** This study is jointly funded by the National Basic Research Program of China (Grant No. 2010CB951102 and 2013CB036406) and the Innovation Research Group Foundation Program of Natural Science Foundation of China (Grant No. 51109224). We are also very grateful to the National Climate Center of China Meteorological Administration for providing all the data used in the study. Last but not the least, many thanks are given to two anonymous reviewers for their valuable comments.

## References

- Akritis MG, Murphy SA, Lavalley MP (1995) The Theil-Sen estimator with doubly censored data and applications to astronomy. *J Am Stat Assoc* 90:170–177
- Bartholy J, Pongrácz R (2007) Regional analysis of extreme temperature and precipitation indices for the Carpathian Basin from 1946 to 2001. *Glob Planet Chang* 57:83–95
- Bartholy J, Pongrácz R (2010) Analysis of precipitation conditions for the Carpathian Basin based on extreme indices in the 20th century and climate simulations for 2050 and 2100. *Phys Chem Earth A/B/C* 35: 43–51
- Bielec Z (2001) Long-term variability of thunderstorms and thunderstorm precipitation occurrence in Cracow, Poland, in the period 1896–1995. *Atmos Res* 56:161–170
- Böhm R, Auer I, Brunetti M, Maugeri M, Nanni T, Schöner W (2001) Regional temperature variability in the European Alps: 1760–1998 from homogenized instrumental time series. *Int J Climatol* 21:1779–1801
- Cao L-J, Yan Z-W (2012) Progress in research on homogenization of climate data. *Adv Clim Chang Res* 3:59–67
- Cavalcanti IFA (2012) Large scale and synoptic features associated with extreme precipitation over South America: a review and case studies for the first decade of the 21st century. *Atmos Res* 118:27–40
- Climate Change (2007) IPCC Fourth Assessment Report. The Physical Science Basis
- Coles S, Casson E (1998) Extreme value modelling of hurricane wind speeds. *Struct Saf* 20:283–296
- Coles S, Pericchi LR, Sisson S (2003) A fully probabilistic approach to extreme rainfall modeling. *J Hydrol* 273:35–50

- Dash SK, Sharma N, Pattnayak KC, Gao XJ, Shi Y (2012) Temperature and precipitation changes in the north-east India and their future projections. *Glob Planet Chang* 98–99:31–44
- Dodla VBR, Ratna SB (2010) Mesoscale characteristics and prediction of an unusual extreme heavy precipitation event over India using a high resolution mesoscale model. *Atmos Res* 95:255–269
- Du H, Xia J, Zeng S (2014) Regional frequency analysis of extreme precipitation and its spatio-temporal characteristics in the Huai River Basin, China. *Nat Hazards* 70:195–215
- Easterling DR, Evans JL, Groisman PY et al (2000) Observed variability and trends in extreme climate events. *Bull Am Meteorol Soc* 72: 1507–1520
- Frank J, Masse J (1951) The Kolmogorov–Smirnov Test for goodness of fit. *J Am Stat Assoc* 46:68–78
- Fu G, Yu J, Yu X, Ouyang R, Zhang Y, Wang P, Liu W, Min L (2013) Temporal variation of extreme rainfall events in China, 1961–2009. *J Hydrol* 487:48–59
- Gaffin SR, Rosenzweig C, Xing X, Yetman G (2004) Downscaling and geo-spatial gridding of socio-economic projections from the IPCC Special Report on Emissions Scenarios (SRES). *Glob Environ Chang* 14:105–123
- Gellens D (2002) Combining regional approach and data extension procedure for assessing GEV distribution of extreme precipitation in Belgium. *J Hydrol* 268:113–126
- Goudie AS (2006) Global warming and fluvial geomorphology. *Geomorphology* 79:384–394
- Griffiths G, Salinger M, Leleu I (2003) Trends in extreme daily rainfall across the South Pacific and relationship to the South Pacific Convergence Zone. *Int J Climatol* 23:847–869
- Groisman PY, Knight RW, Zolina OG (2013) 5.03 - Recent trends in regional and global intense precipitation patterns. In: Pielke RA (ed) *Climate vulnerability*. Academic Press, Oxford, pp 25–55
- Hamed K (2009) Exact distribution of the Mann–Kendall trend test statistic for persistent data. *J Hydrol* 365:86–94
- Haylock M, Nicholls N (2000) Trends in extreme rainfall indices for an updated high quality data set for Australia, 1910–1998. *Int J Climatol* 20:1533–1541
- Hidalgo-Muñoz JM, Argüeso D, Gámiz-Fortis SR, Esteban-Parra MJ, Castro-Diez Y (2011) Trends of extreme precipitation and associated synoptic patterns over the southern Iberian Peninsula. *J Hydrol* 409:497–511
- Hirsch RM, Slack JR, Smith RA (1982) Techniques of trend analysis for monthly water quality data. *Water Resour Res* 18:107–121
- Jenkinson AF (1955) The frequency distribution of the annual maximum (or minimum) values of meteorological elements. *Q J R Meteorol Soc* 81:158–171
- Jhajharia D, Yadav BK, Maske S, Chattopadhyay S, Kar AK (2012) Identification of trends in rainfall, rainy days and 24h maximum rainfall over subtropical Assam in Northeast India. *Compt Rendus Geosci* 344:1–13
- Khaliq M, Ouarda T, Ondo J-C, Gachon P, Bobée B (2006) Frequency analysis of a sequence of dependent and/or non-stationary hydro-meteorological observations: a review. *J Hydrol* 329:534–552
- Kunkel KE, Andsager K, Easterling DR (1999) Long-term trends in extreme precipitation events over the conterminous United States and Canada. *J Clim* 12(8):2515–2527
- Li ZX, He YQ, Theakstone WH, Wang XF, Zhang W, Cao WH, Du JK, Xin HJ, Chang L (2011) Altitude dependency of trends of daily climate extremes in southwestern China, 1961–2008. *Acta Geograph Sin* 22(3):416–430
- Liu Q, Yang Z, Cui B (2008) Spatial and temporal variability of annual precipitation during 1961–2006 in Yellow River Basin, China. *J Hydrol* 361:330–338
- Lu F, Wang H, Yan D, Zhang D, Xiao W (2013) Application of profile likelihood function to the uncertainty analysis of hydrometeorological extreme inference. *Sci China Technol Sci* 56:3151–3160
- Mann HB (1945) Non-parametric test against trend. *Econometrica* 13: 245–259
- Manton M, Della-Marta P, Haylock M, Hennessy K, Nicholls N, Chambers L, Collins D, Daw G, Finet A, Gunawan D (2001) Trends in extreme daily rainfall and temperature in Southeast Asia and the South Pacific: 1961–1998. *Int J Climatol* 21:269–284
- Martinez CJ, Maleski JJ, Miller MF (2012) Trends in precipitation and temperature in Florida, USA. *J Hydrol* 452:259–281
- Nogaj M, Parey S, Dacunha-Castelle D (2007) Non-stationary extreme models and a climatic application. *Nonlinear Process Geophys* 14: 305–316
- Pittock B, Abbs D, Suppiah R, Jones R (2006) Climatic background to past and future floods in Australia. *Floods in an arid continent*:13–39
- Salinger M, Griffiths G (2001) Trends in New Zealand daily temperature and rainfall extremes. *Int J Climatol* 21:1437–1452
- Shao M, Gong Z, Xu X (2013) Risk assessment of rainstorm and flood disasters in China between 2004 and 2009 based on gray fixed weight cluster analysis. *Natural Hazards*:1–28
- Sheffield J, Wood EF (2008) Projected changes in drought occurrence under future global warming from multi-model, multi-scenario, IPCC AR4 simulations. *Clim Dyn* 31:79–105
- Stock CA, Alexander MA, Bond NA, Brander KM, Cheung WWL, Curchitser EN, Delworth TL, Dunne JP, Griffies SM, Haltuch MA, Hare JA, Hollowed AB, Lehodey P, Levin SA, Link JS, Rose KA, Rykaczewski RR, Sarmiento JL, Stouffer RJ, Schwing FB, Vecchi GA, Werner FE (2011) On the use of IPCC-class models to assess the impact of climate on Living Marine Resources. *Prog Oceanogr* 88:1–27
- Suppiah R, Hennessy KJ (1998) Trends in total rainfall, heavy rain events and number of dry days in Australia, 1910–1990. *Int J Climatol* 18: 1141–1164
- Tian Y, Xu Y-P, Boojj M, Lin S, Zhang Q, Lou Z (2012) Detection of trends in precipitation extremes in Zhejiang, east China. *Theor Appl Climatol* 107:201–210
- Tramblay Y, Badi W, Driouech F, El Adlouni S, Neppel L, Servat E (2012) Climate change impacts on extreme precipitation in Morocco. *Glob Planet Chang* 82–83:104–114
- Wang W, Chen X, Shi P, Van Gelder P (2008) Detecting changes in extreme precipitation and extreme streamflow in the Dongjiang River Basin in southern China. *Hydrol Earth Syst Sci* 12(1):207–221
- Wang W, Shao Q, Peng S, Zhang Z, Xing W, An G, Yong B (2011) Spatial and temporal characteristics of changes in precipitation during 1957–2007 in the Haihe River basin, China. *Stoch Env Res Risk A* 25:881–895
- Wang B, Zhang M, Wei J, Wang S, Li X, Li S, Zhao A, Li X, Fan J (2013a) Changes in extreme precipitation over Northeast China, 1960–2011. *Quat Int* 298:177–186
- Wang BL, Zhang MJ, Wei JL, Wang SJ, Li SS, Ma Q, Li XF, Pan SK (2013b) Change in extreme events of temperature and precipitation over Xinjiang, Northwest China, during 1960–2009. *Quat Int* 298: 141–151
- Wang W, Shao Q, Yang T, Peng S, Yu Z, Taylor J, Xing W, Zhao C, Sun F (2013c) Changes in daily temperature and precipitation extremes in the Yellow River Basin, China. *Stoch Env Res Risk A* 27:401–421
- Xia J, She DX, Zhang YY, Du H (2011) Spatio-temporal trend and statistical distribution of extreme precipitation events in Huaihe River Basin during 1960–2009. *J Geogr Sci* 22(2):195–208
- Yan D, Wu D, Huang R, Wang L, Yang G (2013) Drought evolution characteristics and precipitation intensity changes during alternating dry-wet changes in the Huang-Huai-Hai River basin. *Hydrol Earth Syst Sci Discuss* 10
- Yang Z, Yan Y (2006) Research and development of self-organizing maps algorithm. *Comput Eng* 32:201–228
- You QL, Kang SC, Aguilar E, Pepin N, Flügel WA, Yan YP, Xu YW, Zhang YJ, Huang J (2011) Changes in daily climate extremes

- in China and its connection to the large scale atmospheric circulation during 1961–2003. *Clim Dyn* 36(11–12):2399–2417
- Zhai PM, Zhang XB, Wan H, Pan XH (2005) Trends in total precipitation and frequency of daily precipitation extremes over China. *J Clim* 18: 1096–1108
- Zhang Q, Xu CY, Chen X, Zhang Z (2011) Statistical behaviours of precipitation regimes in China and their links with atmospheric circulation 1960–2005. *Int J Climatol* 31:1665–1678
- Zhang Q, Singh VP, Li J, Jiang F, Bai Y (2012) Spatio-temporal variations of precipitation extremes in Xinjiang, China. *J Hydrol* 434–435:7–18